Run-to-Run Control of Membrane Filtration Processes

Jan Busch, Andreas Cruse, and Wolfgang Marquardt
Lehrstuhl für Prozesstechnik, RWTH Aachen University, Turmstraße 46, D-52064 Aachen, Germany

DOI 10.1002/aic.11221
Published online July 23, 2007 in Wiley InterScience (www.interscience.wiley.com).

Membrane filtration processes are often operated cyclically, where one cycle comprises a filtration and a backwashing phase. Due to the complex mechanisms involved, these processes are mostly operated with fixed values of the manipulated variables, leaving much of the economical potential unexplored. A model-based run-to-run process control approach is introduced, in which the manipulated variables are optimized after each filtration cycle. The approach is evaluated in a case study on submerged membrane filtration in wastewater treatment. A simple, computationally inexpensive process model is developed. The resulting model-based controller is tested in a simulation environment employing a validated reference model. It yields excellent results with respect to prediction quality and optimization results. © 2007 American Institute of Chemical Engineers *AIChE J*, 53: 2316–2328, 2007
Keywords: process control, membrane separations, solid/liquid separations, mathematical modeling, optimization

Introduction

This article addresses the model-based control of membrane filtration processes. The approach has originally been developed for the special application of submerged membrane filtration for wastewater treatment. However, the underlying principles have been generalized to apply to the large class of cyclically operated membrane filtration processes. Possibly, even more process types with similar characteristics, such as classical filtration and adsorption processes, could be covered. The distinctive process characteristic is its cyclic operation, where each cycle comprises a filtration (production) and a backwashing (regeneration) phase. The model-based control approach presented in this article exploits this structure in order to operate the respective process safely in the presence of disturbances always close to its economical optimum. Compared to standard operational strategies with fixed set-points, this yields a substantial increase in reliability and economical benefit.

In the following, an introduction to membrane filtration, its control, and its modeling is given. The proposed control approach is motivated and briefly outlined.

Membrane filtration

Membrane filtration is employed to separate particles from a feed fluid. Particles may refer to solid particles, colloids, macromolecules or molecules. A transmembrane pressure difference (TMP) forces the fluid and smaller particles through the membrane pores. They leave the system as *permeate*, while larger particles are retained on the feed side. Filtration applications are operated either in dead end mode with the feed flow parallel to the membrane pores, or in cross-flow mode with the feed flow perpendicular to the pores. Figure 1 (right) shows a hollow-fiber membrane, where the feed is on the outside and the permeate is drawn across the porous walls to the inside. Figure 1 (left) shows many membranes combined into a submerged membrane module. The cross-flow is generated by air bubbles induced at the bottom of the module. The bubbles rise upward, creating a two-phase flow along the membrane surface. The membranes are sealed at

Correspondence concerning this article should be addressed to W. Marquardt at marquardt@lpt.rwth-aachen.de.
Current address of A. Cruse: Uhde GmbH, Friedrich-Uhde-Str. 15, D-44141 Dortmund, Germany. e-mail: andreas@fluor.com

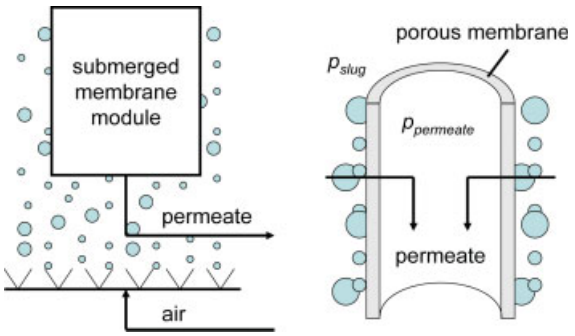

Figure 1. Submerged membrane filtration, TMP = Δp = $p_{slug} - p_{permeate}$

[Color figure can be viewed in the online issue, which is available at www.interscience.wiley.com.]

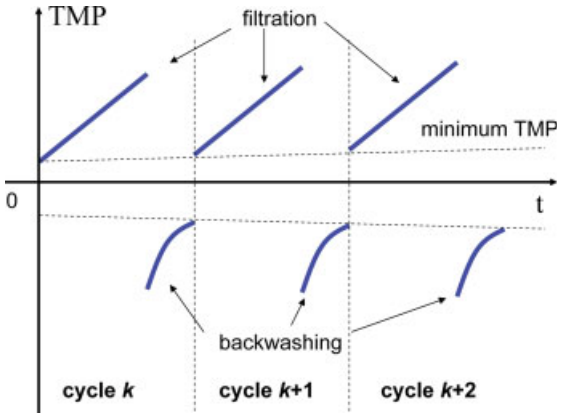

Figure 2. Evolution of the TMP during filtration and backwashing.

During filtration, the TMP rises due to fouling. During backwashing, the absolute value of the TMP decreases due to the removal of fouling effects. The minimum TMP rises due to irreversible fouling. [Color figure can be viewed in the online issue, which is available at www.interscience.wiley.com.]

the top, and the TMP is created by a pump connected to the permeate outlet.

The permeability of the membranes and therefore the filtration performance decreases with time due to *membrane fouling*. Many mechanisms contribute to membrane fouling, and their relative importance depends on the specific process. In most applications, the repelled particles concentrate on the feed side of the membrane and build a filter cake (*organic fouling*). Furthermore, pores are blocked by intruding particles (*pore blocking*). Microorganisms build biofilms on the membrane and pore surfaces, which decrease the performance and potentially damage the membrane (*biofouling*). When inorganic soluble substances are repelled by the membrane, they concentrate on the feed side of the membrane, and after reaching the limit of solubility, they crystallize and add to cake layer formation (*scaling, inorganic fouling*). The concentration gradient of retained substances induces backdiffusion away from the membrane (*concentration polarization*). All of these phenomena reduce the process efficiency and can be counteracted by membrane and module design, as well as by appropriate process control strategies.

There are three main concepts for limiting membrane fouling during operation. First, cross-flow along the membrane surface decreases the deposition of substances. Second, during backwashing phases the flow direction through the membrane is reversed, such that the membrane pores are flushed with permeate. The third measure is to chemically or mechanically clean the membranes, which is usually performed at a much lower frequency than the other two measures. Each of these measures reduces membrane fouling, however, all of them increase the operational cost due to energy consumption, loss of product and availability, and the cost of cleaning agents. While cross-flow intensity and backwashing are optimized by the control algorithm proposed in this article, mechanical and chemical cleanings are not taken into account due to their low frequency.

Figure 2 shows the typical, yet simplified evolution of the TMP for three filtration cycles, assuming that a constant filtration and backwashing flux is applied. Each filtration cycle consists of a filtration phase (positive TMP) followed by a backwashing phase (negative TMP). During filtration, the TMP increases mainly due to cake layer formation. After a fixed filtration time, the flux is reversed and the membrane is cleaned. Due to the removal of the cake layer and the clearing of the pores, the absolute value of the TMP decreases with time. The minimum TMP at the beginning of the filtration cycles also increases with time, as membrane fouling is not completely reversed by backwashing.

Process control of membrane filtration

Filtration systems realize a certain permeate flux J, which is the permeate volume flow per membrane area. The net flux J_{net} of a membrane filtration system is defined as

$$J_{\text{net}} = \frac{J_f \cdot \Delta t_f - J_b \cdot \Delta t_b}{\Delta t_f + \Delta t_b}, \tag{1}$$

where J_f and J_b are the filtration and the backwashing fluxes and Δt_f and Δt_b are the filtration and backwashing phase durations, respectively. Typically J_f, J_b, Δt_f, and Δt_b are operational degrees of freedom. In cross-flow systems, the cross-flow intensity u_c is available as a fifth degree of freedom. It is assumed in the following, that the desired net flux J_{net} is determined by an upper-level controller or operator.

In industrial practice today filtration processes are usually controlled by fixing J_f, J_b, Δt_f, Δt_b, and u_c to constant values such that the desired net flux is realized and fouling is kept within reasonable limits. The choice of these values is made according to a pre-specified scheme or to the operator's experience. The reason for the rather simple control approach is the high complexity of the filtration process. It is characterized by the periodic change between filtration and backwashing, by the drift of membrane permeability due to irreversible membrane fouling, and by a high-number of disturbances, including variations of temperature or solids concentration. Furthermore, only very limited measurement information is available in industrial installations. In most cases, only the overall TMP across an entire membrane module is measured.

There are some approaches in the literature to better the performance of membrane filtration systems by understanding the influence of the controls during operation and adapting them accordingly. Most of them are based on experimen-

tal setups which analyze the effect of altering, e.g. the cross-flow characteristics,[1] the mechanical and chemical cleaning frequencies,[2] or the filtration phase duration and the filtration flux.[3] Another research direction is the development of mechanistic models of the filtration process and performing simulation experiments, which again give insight into the effects of the various controls.[4,5] Smith et al.[6] present an online approach in which backwashing is initiated when the TMP has increased by a certain amount, which is advantageous as compared to backwashing at a fixed frequency. Finally, Blankert et al.[7] develop a filtration model and determine the optimal profile of the filtration flux and TMP during one filtration phase using offline dynamic optimization. They find that constant flux filtration, which is typically performed in industrial applications, is indeed close to optimal performance concerning energy consumption.

Membrane filtration modeling

Model-based control is oftentimes employed to increase the performance of industrial processes with respect to reliability and economic performance. The quality of any model-based controller depends on the process model employed. Rigorous, mechanistic modeling of filtration processes is a highly complex task due to the many physical and possibly chemical and biological phenomena, which take place on very different time scales. Still, there are several approaches available in the literature for different applications and membrane types. Most of them are based on Darcy's law $\Delta p = J \cdot \eta \cdot R$, where J is the flux, η is the fluid viscosity, and R is the membrane resistance. They differ in the level of detail and local resolution with which the resistance R is described. Busch et al.[4] and Broeckmann et al.[8] present a model covering pore blocking, filter cake and biofilm formation, polydispersed particles, and gas-liquid feed flow along the membrane length axis for submerged hollow-fiber membranes. Polyakov[9] focuses on dead end hollow-fiber filtration, and cushion modules are comprehensively treated by Gehlert et al.[10] More general modeling approaches for various types of membranes and applications are described by Marriott and Sørensen[11,12] and Mangold et al.[13]

However, there are also many approaches based on simple semi-empirical laws describing the temporal evolution of fouling[14] or on purely data driven neural networks.[15–17]

From a model-based process control point of view, both simple and complex models of either empirical or mechanistic nature have advantages and drawbacks. More complex models can yield a higher prediction quality, however, they typically employ many parameters which are difficult to determine offline or require much online measurement data. Simpler modeling approaches require less measurement data for identification and little computational time, but suffer from low-prediction quality, especially on longer time horizons. Given the high uncertainty and little measurement information available in industrial filtration processes, simple models present a more intuitive choice for control purposes and are therefore employed in this work.

Outline of this article

The key idea pursued throughout this article is the following: A simple model is required to fulfill the online requirements of low-computational cost and sufficient identifiability. The low-prediction quality of the simple model is increased by frequently adapting the model to plant measurements. The filtration process is divided into cycles, and each cycle is divided into a filtration and a back-washing phase. The operation of the filtration process can then be represented as a continuous sequence of cycles. This structure is exploited by updating the process model after each cycle based on the newly available measurement data. The updated model is employed to determine the optimal set-points for the manipulated variables for the next cycle. This strategy is known as *run-to-run control*.

In the following section, the run-to-run control theory is briefly introduced, and it is then extended to the class of cyclically operated processes with filtration (production) and backwashing (regeneration) phases. This provides the framework to develop model-based controllers for specific applications. The approach is exemplified in a case study, in which a suitable model for submerged membrane filtration for wastewater treatment is developed. The resulting model-based controller is evaluated in a simulation study. Finally, conclusions are drawn and current research topics are highlighted.

Run-to-Run Control for Membrane Filtration

In this section, the framework for run-to-run control of membrane filtration processes is developed. First, the general run-to-run control theory is briefly revisited. It is then extended to account for the characteristics of membrane filtration processes, mainly the circumstance that one run (cycle) comprises two phases. Related issues as the dual control problem, the treatment of unidentifiable parameters, the certainty equivalence principle, and the impact of computational delay are discussed.

Run-to-run control

Run-to-run (or run-by-run, batch-to-batch) process control has originally been proposed for semi-conductor manufacturing processes, where silicon wafers are produced in batches. While continuous PID-type controllers are employed *during* the batches, the run-to-run controller is only active *between* the batches. The run-to-run controller calculates the set-points for the manipulated variables, which are then realized by PID-type controllers. The calculation of the optimal set-points is based on a simple process model, which is updated using the measurements from the previous batch. Figure 3 illustrates the embedding of the run-to-run controller in the control system, where $\mathbf{u}$ are the set-points for the manipulated variables as computed by the run-to-run controller, $\mathbf{v}$ the outputs from the base controller, $\mathbf{y}$ the measurements, $\mathbf{p}$ the parameters and initial states, and ϕ the objective function of the control problem. An extensive review on run-to-run control is provided by del Castillo and Hurwitz.[18]

Much of the fundamental work on run-to-run control has been developed for single-input single-output (SISO) processes, which can be described by the linear stationary model

$$y^k = \alpha + \beta \cdot u^{k-1} + \epsilon^k, \tag{2}$$

where k indexes the run (batch), ε represents the model error often assumed to be white noise, and α and β are model

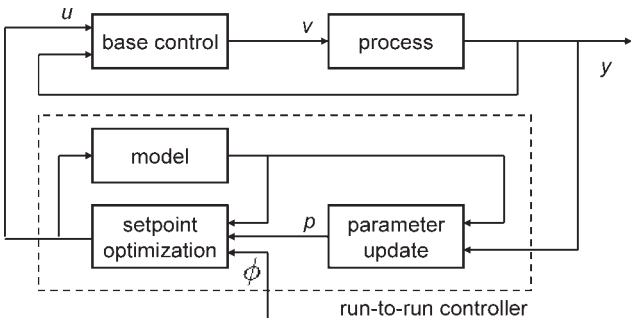

Figure 3. Run-to-run control.

parameters. Let r be the set-point of y. If α and β were constants, the perfect feedforward control law

$$u^k = \frac{r - \alpha}{\beta} \tag{3}$$

could be implemented. If however the process is disturbed, e.g. due to aging of equipment or changes in the feed composition, this simple approach will not yield optimal process performance. Instead, the model parameters need to be adapted and a new value u^k for the manipulated variable needs to be calculated for every run (batch) according to Figure 3.

Several strategies have been proposed for the update of the model parameters, depending on the properties of the process and of the chosen process model. They include exponentially weighted moving average (EWMA) filters, double EWMA, least-squares parameter estimation, and many more.[18–23] Usually the measurements from the previous run (batch) $k - 1$ are used to compute an estimate of the parameters for run (batch) k, e.g. α^k and β^k for the SISO model given in Eq. 2. The manipulated variable u^k for batch k is then computed from

$$u^k = \frac{r - \alpha^k}{\beta^k}. \tag{4}$$

Run-to-run control for membrane filtration

For the filtration systems treated in this article, a more general problem formulation is required. In the following, a general framework for the run-to-run control of membrane filtration processes is developed, from which individual controllers for specific applications and purposes can be derived. This is exemplified in the case study presented in the next section. Several variations of the run-to-run principle have been proposed in the past. Recent examples are the control of batch chromatography,[23] yeast fermentation,[24] and batch polymerization.[25] Srinivasan et al.[26] reduce the dynamic optimization problem within a run-to-run scheme to a control problem by tracking online the previously determined necessary conditions of optimality. François et al.[27] apply this concept to a batch polymerization process.

In contrast to the approaches mentioned earlier, a run-to-run scheme for filtration processes has to account for the fact that each filtration cycle, or run, is divided into a filtration and a backwashing phase. The estimation and control horizons are each divided into a sequence of two phases, for each of which different models are employed. This structure leads to a multistage optimization problem.[28] The problem formulations proposed below are specializations of the more general formulation for this type of problems given by Oldenburg et al.[29] Due to the complexity of the filtration process, the proposed framework allows both phases to be described by nonlinear dynamic models. This implies that in addition to the model parameters, also the initial states of the dynamic model have to be estimated.

In the following, the parameter and state estimation, as well as the control problems are formulated. First, the optimal control problem is presented. To correctly represent the repeated solution of the problem on a moving horizon, the cycle index k should be introduced for every variable. However, to ease the notation, the index k is omitted. The index j is introduced to distinguish the filtration and the backwashing phase, indicated by the value f or b, respectively. The optimization problem for cycle k, which is the analog to Eq. 4 in the linear SISO case, is then

$$\min_{\mathbf{u}_j, t_{j,e}} \phi \tag{P1}$$

$$\text{s.t. } \mathbf{f}_j(\dot{\mathbf{x}}_j, \mathbf{x}_j, \mathbf{y}_j, \mathbf{u}_j, \mathbf{p}_j, \mathbf{d}_j, t) = 0 \tag{5}$$

$$\mathbf{g}_j(\mathbf{x}_j, \mathbf{y}_j, \mathbf{u}_j, \mathbf{p}_j, \mathbf{d}_j, t) \le 0 \tag{6}$$

$$\mathbf{h}_j(\mathbf{x}_j, \mathbf{y}_j, \mathbf{u}_j, \mathbf{p}_j, \mathbf{d}_j, t_{j,e}) \le 0 \tag{7}$$

$$\Gamma(\mathbf{x}_f(t_{f,e}), \mathbf{x}_b(t_{b,0})) = 0 \tag{8}$$

$$\mathbf{x}(t_0) = \mathbf{x}_0 \tag{9}$$

$$t_0 = t_{f,0} \le t_{f,e} = t_{b,0} \le t_{b,e} = t_e \tag{10}$$

$$t \in [t_0, t_e] \tag{11}$$

$$j = \begin{cases} f & \text{for } t \in [t_{f,0}, t_{f,e}] \\ b & \text{for } t \in [t_{b,0}, t_{b,e}]. \end{cases} \tag{12}$$

$\mathbf{x}$ are differential and $\mathbf{y}$ are algebraic state variables, $\mathbf{d}$ are disturbances, and t is the time. ϕ is the objective function representing the operational cost. $\mathbf{f}_j$ is the set of differential-algebraic equations (DAE) of index 1 describing the process. $\mathbf{g}_j$ are path and $\mathbf{h}_j$ are endpoint constraints. Equation 8 gives phase transition conditions $\mathbf{\Gamma}$ between the differential states at the end of the filtration phase and the beginning of the backwashing phase. The consistent initial states of the DAE system are given in Eq. 9. Equations 10–12 define the optimization horizon and the phase durations. The length of one cycle is given by the time interval $[t_0, t_e]$, and comprises the filtration phase $[t_{f,0}, t_{f,e}]$ and the backwashing phase $[t_{b,0}, t_{b,e}]$.

It should be noted that the problem formulation (P1) does not consider the influence of cycle k on cycle $k + 1$. For example, insufficient cleaning in the backwashing phase of cycle k lowers the operational cost in cycle k, but the negative impact on cycle $k + 1$ is not considered. If necessary, appropriate endpoint constraints (Eq. 7) have to be stated, which, e.g., enforce that the final filtration resistance after backwashing is below a certain limit.

The parameter and state estimation problem is formulated in a similar fashion. The initial states $\mathbf{x}_0$ are treated as parameters

and estimated together with the model parameters $\mathbf{p}_j$. With the assumption of white process and measurement noise, the estimation problem reduces to a least-squares optimization problem.[30,31] The formulation must account for the discrete nature of the TMP measurement data, which are sampled at n_l time points $t_l \in [t_0, t_e]$. The predicted TMP measurements are therefore sampled accordingly. Again omitting the cycle index k for better readability, the estimation problem is formulated as

$$\min_{\mathbf{p}_j, \mathbf{x}_0} \sum_{l=1}^{n_l} \frac{1}{2} (\Delta\tilde{p}_{j,l} - \Delta p_{j,l})^2 \tag{P2}$$

$$\text{s.t. } \mathbf{f}_j(\dot{\mathbf{x}}_j, \mathbf{x}_j, \mathbf{y}_j, \mathbf{u}_j, \mathbf{p}_j, \mathbf{d}_j, t) = 0 \tag{13}$$

$$\Delta p_{j,l} = \Delta p_j(t_l) \tag{14}$$

$$\Gamma(\mathbf{x}_f(t_{f,e}), \mathbf{x}_b(t_{b,0})) = 0 \tag{15}$$

$$\mathbf{x}(t_0) = \mathbf{x}_0 \tag{16}$$

$$t_0 = t_{f,0} \leq t_{f,e} = t_{b,0} \leq t_{b,e} = t_e \tag{17}$$

$$t_l \in [t_0, t_e], l \in \{1, \ldots, n_l\} \tag{18}$$

$$j = \begin{cases} f & \text{for } t_l \in [t_{f,0}, t_{f,e}] \\ b & \text{for } t_l \in [t_{b,0}, t_{b,e}]. \end{cases} \tag{19}$$

$\Delta\tilde{p}_{j,l}$ are the sampled measurements of the TMP, whereas $\Delta p_{j,l}$ are the corresponding predicted measurement samples. The solution of (P2) provides updated values of the parameters and the initial values based on the measurements of cycle $k - 1$.

Depending on the process, it might be desirable not to entirely rely on the most recent solution of the estimation problem, which is only based on data from the previous, possibly strongly disturbed cycle. In such situations, filtering the parameter updates is a well proven technique.[32]

Dual control problem

So far it has been assumed that all model parameters $\mathbf{p}$ and initial values $\mathbf{x}_0$ can be estimated using the data from the previous cycle $k - 1$. However, it is not guaranteed that the information content of these measurements is sufficient to reliably identify all unknown quantities. Missing excitation of certain states, inputs or disturbances might lead to an estimation problem in which not all of the unknowns are independently identifiable. This is referred to as the *dual control problem*.[33] To illustrate the problem, consider the model

$$y(t) = \alpha \cdot u(t)^{\beta}, t_1 \leq t \leq t_2. \tag{20}$$

If $u(t)$ is constant on the entire estimation horizon, which might comprise several cycles, then $y(t)$ is also constant, and α and β cannot be estimated independently. Consider, e.g. $u(t) = 3$ and $y(t) = 5$, then there is an infinite number of solutions for α and β, which satisfy Eq. 20. To overcome the problem, either $u(t)$ has to be excited, which might lead to a decrease in performance, or the estimation horizon has to be chosen large enough to include a natural variation in $u(t)$.

The dual control problem does affect the proposed model-based run-to-run controller. This is due to the fact that the inputs of the filtration process are usually constant within one filtration cycle, which means that they are not excited on the estimation horizon. Therefore, an estimation technique is proposed, which exploits relationships from stochastics and parameter estimation theory.[30] It enables the reliable estimation of the affected parameters and initial values on appropriately chosen longer time horizons $[t_0^{k-N}, t_e^{k-1}]$, where N is the number of filtration cycles considered. To ease the notation, the following approach is formulated for the parameters $\mathbf{p}_j$ only, but it applies likewise for the initial values $\mathbf{x}_0$.

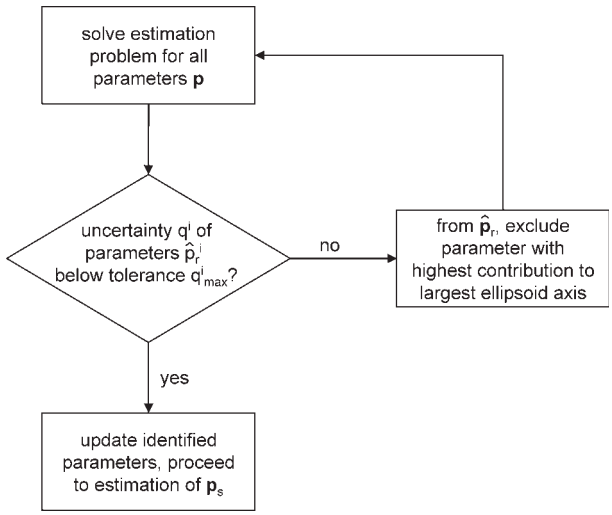

Figure 4. Parameter estimation on longer time horizons.

The parameters $\mathbf{p}$ are divided into a set of parameters $\mathbf{p}_s = \{p_s^1, \ldots, p_s^i, \ldots, p_s^{n_s}\}$, which are estimated on the data of one filtration cycle according to (P2), and a second set of parameters $\mathbf{p}_r = \{p_r^1, \ldots, p_r^i, \ldots, p_r^{n_r}\}$, which as a consequence are not identifiable on the same horizon due to the dual control problem.

The estimation algorithm for the parameters $\mathbf{p}_r$ is depicted in Figure 4. First, the estimation problem is solved for all parameters analogously to (P2), but on the horizon $[t_0^{k-N}, t_e^{k-1}]$. When the estimation problem has converged to a solution $\hat{\mathbf{p}}$, the quality of the estimates is evaluated. The Hessian $\mathbf{H}$ at the solution describes a confidence ellipsoid in the parameter space given by

$$\delta\mathbf{p}^T \cdot \mathbf{H} \cdot \delta\mathbf{p} \leq 2 \cdot \varepsilon, \tag{21}$$

where ε is a parameter defining the size of the so-called indifference region, and $\delta\mathbf{p}$ is a vector of deviations from the optimal parameter values $\hat{\mathbf{p}}$. Eq. 21 states how much the parameters may be changed under the condition that the objective function value does not change more than ε. Let λ^j be an eigenvalue and $\mathbf{v}^j$ the corresponding unit eigenvector of the Hessian $\mathbf{H}$, $j \in \{1, \ldots, n_p\}$, where n_p is the number of parameters, and where the eigenvalues are sorted in increasing order. Then, the length l^j of the corresponding main axis of the confidence ellipsoid is

$$l^j = \sqrt{\frac{2 \cdot \varepsilon}{\lambda^j}} \tag{22}$$

and the axis $\mathbf{a}^j$ is given by

$$\mathbf{a}^j = \mathbf{v}^j \cdot l^j. \tag{23}$$

The longer the ellipsoid extends in the direction of one parameter, the smaller is the confidence into the corresponding estimated value. Therefore, the maximum extension of all main axes in the direction of a parameter p^i is taken as an uncertainty measure q^i of parameter p^i according to

$$q^i = \max\left(a_i^j\right),\ \forall j \in \{1,\ldots,n_p\}, \tag{24}$$

where a_i^j is the ith element of $\mathbf{a}^j$. It should be noted that since the main axes are in general not parallel to the coordinate axes, the maximum extension of the main axes is not exactly equal to the extension of the ellipsoid itself. However, this deviation is small compared to the absolute value and is neglected in the following. It needs to be ensured that the uncertainty of the parameter estimates $\hat{\mathbf{p}}_r$ is below a certain threshold, if they are to be adopted. If not all of the parameter estimates $\hat{\mathbf{p}}_r$ have uncertainty measures below a specific tolerance $q^i_{\max}$, the parameter with the highest contribution to the largest ellipsoid axis is excluded from the estimation problem, and the reduced estimation problem is solved again. This procedure is repeated until a subset of the parameters $\mathbf{p}_r$ is estimated within the specified tolerances, or until all parameters have been excluded from the estimation problem. Newly identified parameter values are adopted, while the previously excluded parameters keep their initial values. The number of filtration cycles N, the indifference region parameter ε, and the uncertainty tolerances $q^i_{\max}$ are tuning parameters.

After the estimation of the parameters $\mathbf{p}_r$, the estimation of the remaining parameters $\mathbf{p}_s$ with the data from the previous filtration cycle $k-1$ is performed according to (P2).

Certainty equivalence principle

Since the control problem (P1) depends on the estimated parameters $\mathbf{p}_j$ and the estimation problem (P2) depends on the measurements $\tilde{\mathbf{y}}_{j,l}$, which in turn depend on the optimized manipulated variables $\mathbf{u}_j$, both problems are interdependent. This in turn implies that the control algorithm depicted in Figure 3 is not guaranteed to converge to optimal process performance. In fact, it can be shown that it will only lead to optimal performance if the gradient of the measurements with respect to the manipulated variables of the real process equals the according gradient of the prediction, i.e.

$$\frac{\partial \tilde{\mathbf{y}}^k_{j,l}}{\partial \mathbf{u}^k_j} = \frac{\partial \mathbf{y}^k_{j,l}}{\partial \mathbf{u}^k_j}, \tag{25}$$

which is most likely not the case in practice. Roberts[34] was the first to address this problem systematically (see Roberts[35] for a review and Gao and Engell[23] and Xiong and Zhang[25] for recent applications). Most of the proposed strategies to circumvent the problem are based on the estimation of the gradient $\partial \tilde{\mathbf{y}}^k_{j,l}/\partial \mathbf{u}^k_j$ from process measurements and a subsequent modification of the control problem. Within the scope of this paper, this problem is not considered. The estimated parameters are taken as the correct parameters, a common assumption known as the *certainty equivalence principle*. The induced error is expected to be small against other disturbances, however, a rigorous method to estimate the error is not available.

Computational delay

The control algorithm comprises three steps: parameter and initial value estimation using data from a long horizon, parameter and initial value estimation using data from the last cycle, and optimization of the manipulated variables for the future cycle. Ideally, the estimation and optimization take place between two cycles $k-1$ and k, and the optimized manipulated variables are realized at the beginning of the new cycle k (Figure 5). However, since there is no pause in between the two cycles, zero calculation time would be required. Hence, a delay in the implementation of the optimized manipulated variables is inevitable. Different strategies are available to handle the delay. One option is to delay the implementation by an entire cycle, thereby providing plenty of time for communication and solution of the estimation and optimization problems. Alternatively, the solution is implemented as soon as it is available in cycle k, accepting the delay in the implementation of the manipulated variables. However, any delay can possibly lead to a loss of stability of the closed-loop control system.[36] In the online implementation of the proposed control scheme at an industrial pilot plant, which is currently examined, the optimized manipulated variables are realized with one cycle delay, and no stability problems have been observed so far.

Case study: Submerged Microfiltration for Wastewater Treatment

The proposed run-to-run control framework is generic for membrane filtration applications which are operated cyclically, with each cycle comprising a filtration and a backwashing phase. Beyond that, there are many more processes which exhibit similar characteristics, e.g. classical filtration and adsorption, and to which the framework might apply. The framework allows to derive controllers for specific applications and purposes, if a suitable process model is available. In the following, the controller design is exemplified step by step for submerged microfiltration (MF) with intermitted aeration for wastewater treatment applications in order to highlight the procedure and demonstrate the effectiveness of the

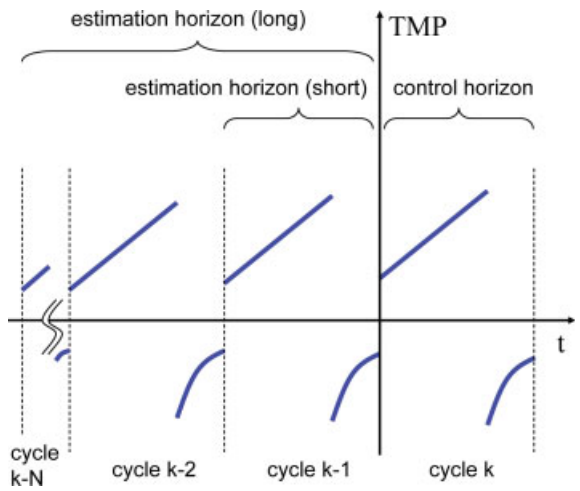

Figure 5. Run-to-run control for membrane filtration.

[Color figure can be viewed in the online issue, which is available at www.interscience.wiley.com.]

approach. First, the process is described. A suitable model is developed, including the objective function and process constraints. Finally, the resulting controller is formulated and tested in simulation.

Process description

Wastewater treatment represents a large industry with high annual product volume, as well as financial investments.[37] Shrinking water resources lead to intensified water reuse and increasingly strict legislative limits on effluent concentrations. At the same time, economical pressure demands for efficient process solutions. Membrane bioreactors (MBR) represent one promising technology in this context.[38] In conventional wastewater treatment plants, the biomass is separated from the effluent in sedimentation basins. In MBR, the basins are replaced by membrane filtration. In most cases, submerged low-pressure MF membranes are employed due to their low specific cost.[39] The advantages of MBR include high effluent purity, small plant size, and high biomass concentrations. Today MBR are already profitable in the upgrading of existing plants and in environments with high effluent purity demands. Due to continuous technological advances with respect to the design and operation of MBR and stricter effluent requirements, MBR are expected to play an increasingly important role in wastewater treatment.[40–42]

The feed to the MBR consists of water, in which a variety of organic and inorganic particles and dissolved substances are present. Organic fouling, biofouling, and pore blocking are the dominating fouling effects. Usually hollow-fiber membranes or plate modules with nominal pore sizes around one micron or less are employed. The cross-flow is realized with air bubbles periodically injected at the bottom of the modules.

Process model for control

In order to study the highly complex process, a rigorous model has been developed, which is discussed in detail by Busch et al.[4] and Broeckmann et al.[8] It has been shown to adequately represent real plant behavior and is therefore used as a reference model in the following simulation study. For the run-to-run control framework, a much simpler model is formulated, including a suitable objective function and process constraints.

The model proposed in the following is based on very simple descriptions of the main phenomena occurring in the filtration process. The differential equations involved can be solved analytically, allowing a very efficient online computation. The transmembrane pressure difference Δp is described by Darcy's law

$$\Delta p = J \cdot \eta \cdot R, \tag{26}$$

where J is the flux, η is the fluid viscosity, and R is the membrane resistance. While J is a manipulated variable, η depends on the feed suspension properties. It can either be derived from an empirical correlation if further measurements, e.g., of the temperature and of the solids concentration are available (e.g., Lübbecke and Vogelpohl[43]), or it can be set to a constant typical value. As the TMP is assumed to be measurable, Eq. 26 represents the system's output equation. In the following, a filtration and a backwashing model are introduced, which describe the resistance R.

Filtration Phase. During filtration, the membrane resistance R_f is described by

$$\frac{dR_f}{dt} = m \cdot J_{f^\alpha} \cdot u_c^\beta \tag{27}$$

$$R_f(t_{f,0}) = R_f^0. \tag{28}$$

R_f^0 is the initial membrane resistance. m, α, and β are model parameters. $\alpha > 0$ holds, because high fluxes J_f lead to an increase in membrane resistance. Accordingly, $\beta < 0$ has to hold to account for the strong increase of filtration resistance related to low cross-flow intensity. If the filtration flux J_f and the cross-flow intensity u_c are constants, a linear increase of membrane resistance results. It describes the cake layer formation, which is the dominating effect on this time-scale.

The filtration model is very simple and combines some physical insight about relevant effects with an empirical correlation. Obviously, this model will only yield sufficient prediction quality if the model parameters are frequently adapted to the current process behavior. Note, that Eq. 27 can be solved analytically, facilitating the solution in real-time.

Backwashing Phase. While often a linear increase of membrane resistance can be observed during filtration, its decrease during backwashing is typically exponential and converges to an irreversible resistance R_b^∞ according to

$$\frac{dR_b}{dt} = -\frac{n}{\tau_b} \cdot \Delta R \cdot e^{-(t-t_{b,0})/(\tau_b)} \tag{29}$$

$$R_b(t_{b,0}) = n \cdot \Delta R + R_b^\infty \tag{30}$$

$$\Delta R = R_f(t_{b,0}) - R_b^\infty \tag{31}$$

n and τ_b are model parameters. ΔR is the difference between the final resistance of the filtration phase $R_f(t_{f,e}) = R_f(t_{b,0})$ and the irreversible resistance R_b^∞ (Eq. 31). The initial resistance at the beginning of the backwashing phase $R_b(t_{b,0})$ need not equal the final resistance at the end of the filtration phase $R_f(t_{f,e})$ (Eq. 29), since Darcy's law neither captures the hydrodynamics in the pipes between the membrane and the pump nor the nonlinear dependency of the filtration resistance on the flux, which is observed in real applications.

Cost function. The objective function needs to consider all cost, which are sensitive to the manipulated variables. These are

- the electrical energy to provide the TMP,
- the electrical energy to provide the cross-flow,
- and membrane replacement.

The electrical energy to provide the TMP in cycle k is given by

$$\frac{dE_p}{dt} = \frac{|\Delta p \cdot J_j \cdot A|}{\eta_P \cdot (t_e - t_0)},\ E_p(t_0) = 0, t \in [t_0, t_e] \tag{32}$$

where A is the membrane area, and η_p is the efficiency factor of the permeate pump.

The power required for the cross-flow depends on how the cross-flow is realized. In dead end operation, it is zero. In

classical cross-flow modules, the entire feed flows parallel to the membrane surface. In submerged modules, the cross-flow is usually realized with air bubbles, which are intermittently injected at the bottom of the filtration module and which establish a two-phase flow along the membrane in vertical direction. The cross-flow intensity u_c is not explicitly available as manipulated variable. Rather, it is a function of the constant air flow rate Q, the length of the aerated intervals t_{on}, and the length of the aeration pauses t_{off}. The membrane is always aerated during backwashing to push biomass out of the membrane module. Hence, u_c is defined as

$$u_c = Q \cdot \frac{t_{\text{on}}}{t_{\text{on}} + t_{\text{off}}}, \tag{33}$$

where t_{off} is chosen to be the redefined manipulated variable replacing u_c. The power necessary to supply the air flow can be described as

$$E_c = \frac{Q \cdot T \cdot R_g \cdot \gamma_a \cdot \left[(1+p_a)^{\frac{\gamma_a}{\gamma_a - 1}} - 1\right]}{v_a \cdot (\gamma_a - 1) \cdot \eta_A \cdot t_{b,e}} \times \left(\frac{t_{f,e} \cdot t_{\text{on}}}{t_{\text{on}} + t_{\text{off}}} + (t_{b,e} - t_{f,e})\right), \tag{34}$$

assuming that the compression is a polytropic process. T is the ambient air temperature, v_a is the molar volume of air, R_g is the gas constant, $\gamma_a = 1.4$ is the polytropic coefficient, p_a is the pressure difference across the compressor (in bar), and η_A is an efficiency factor. Eq. 34 assumes that the air compressor operates at constant power, such that the air flow rate Q is the same during filtration and backwashing. Since the air flow Q is not an optimization variable, this assumption could easily be dropped and different values for filtration and backwashing could be used.

The cost for membrane replacement E_r cannot be described as straightforwardly as the energy cost. In fact, there is not yet quantitative insight to describe the influence of the manipulated variables on the membrane lifetime. Depending on the filtration system under consideration, different models for E_r have to be developed. The following model is proposed for MF membranes in wastewater applications. It has been observed in practice that a strong increase of TMP within a filtration cycle indicates an overstraining of the membrane. It is also known that the longer the filtration phase lasts, the more the reversible resistance changes into irreversible resistance, e.g. due to biofilm formation. Therefore, the TMP increase within one filtration phase is penalized, where the penalty increases exponentially with time according to

$$E_r = \xi_1 \cdot (\Delta p(t_{f,e}) - \Delta p(t_{f,0})) \cdot e^{t_{f,e}/\xi_2}. \tag{35}$$

ξ_1 and ξ_2 are tuning parameters, where ξ_1 linearly scales the fouling cost, and where ξ_2 is a time constant. Higher values of ξ_1 and lower values of ξ_2 lead to a conservative mode of operation, where the straining of the membrane is strongly penalized. The lower ξ_1 and the higher ξ_2 are chosen, the more the direct operating cost in terms of energy consumption are minimized.

Table 1. Separation of Model Parameters

Estimation Horizon	Parameter Set	Elements
filtration phase cycle $k-1$	p_s	m, R_f^0
backwashing phase cycle $k-1$	p_s	n, τ_b, R_b^∞
filtration phase cycles $[k-N, k-1]$	p_r	α, β

The overall cost function ϕ is

$$\phi(t_e) = E_p(t_e) + E_c + E_r. \tag{36}$$

Constraints. Process constraints consist of safety relevant state constraints and physical bounds on the manipulated variables. The most important constraint in membrane filtration is the maximum pressure difference across the membrane $\Delta p_{\max}$. The fluxes J_f and J_b and the cross-flow intensity u_c are limited due to physical reasons. Still, tighter limits can be imposed on the fluxes J_f and J_b, the phase durations defined by $t_{f,e}$ and $t_{b,e}$, and the cross-flow intensity u_c in order to safeguard the membrane. All of these constraints can easily be added to the control problem formulation as

$$\Delta p_{\min} \le \Delta p \le \Delta p_{\max} \tag{37}$$

$$\mathbf{u}_{\min} \le \mathbf{u} \le \mathbf{u}_{\max}, \tag{38}$$

where $\mathbf{u}$ comprises the manipulated variables J_f, J_b, $t_{f,e}$, $t_{b,e}$, and t_{off}.

Run-to-run controller

In this section, the estimation and the optimal control problems of the run-to-run controller for submerged membrane filtration are formulated, employing the models derived before.

Estimation. In industrial practice, only the TMP across the membrane module is measured. In order to make the proposed approach widely applicable, it is therefore assumed that only this measurement is available. It is further assumed that the filtration flux J_f, the backwashing flux J_b, and the aeration pauses t_{off} are set to constant values in each cycle and that these set-points are satisfactorily realized by base controllers. This however implies that the parameters m, α, and β cannot be identified independently using the measurement data from one filtration phase (Eq. 27). The estimation problem is, therefore, separated into two subproblems as proposed in the previous section.

The parameters are split into two sets as shown in Table 1. The parameters m, R_f^0, n, τ_b, and R_b^∞ are estimated using the data of the previous cycle $k-1$. The remaining parameters α and β are estimated on longer time horizons.

First, the estimation problem using measurements from cycle $k-1$ is treated. The estimation problems for the filtration and the backwashing phase are coupled through the phase transition condition (Eq. 31), which relates the filtration resistance at the end of the filtration phase to the initial resistance of the backwashing phase. In order to simplify the problem and to decrease the computational demand, they are, however, solved sequentially. The simple model structure allows for an analytical solution of the differential equations.

The initial value and parameter estimation problem for cycle k using the measurement data from cycle $k-1$ for the filtration phase is then

$$\min_{m,R_f^0} \sum_{l=1}^{n_{f,l}} \frac{1}{2}(\Delta\tilde{p}_{f,l} - \Delta p_{f,l})^2 \tag{P3}$$

$$\text{s.t. } \Delta p_{f,l} = J_f \cdot \eta \cdot R_{f,l}, \tag{39}$$

$$R_{f,l} = R_f^0 + m \cdot J_f^{\alpha} \cdot u_c^{\beta} \cdot t_l \tag{40}$$

$$t_l \in [t_0, t_{f,e}],\ l \in \{1, \ldots, n_{f,l}\}, \tag{41}$$

where $\Delta\tilde{p}_{f,l}$ are discrete measurements at the sampling points t_l in cycle $k-1$, and $\Delta p_{f,l}$ are the corresponding predicted measurements.

The backwashing model parameters are estimated from

$$\min_{n,\tau_b,R_b^{\infty}} \sum_{l=n_{f,l}+1}^{n_{b,l}} \frac{1}{2}(\Delta\tilde{p}_{b,l} - \Delta p_{b,l})^2 \tag{P4}$$

$$\text{s.t. } \Delta p_{b,l} = J_b \cdot \eta \cdot R_{b,l} \tag{42}$$

$$R_{b,l} = R_b^{\infty} + \Delta R \cdot n \cdot e^{-(t_l - t_{n_{f,l}})/(\tau_b)} \tag{43}$$

$$\Delta R = R_{f,l}(t_{n_{f,l}}) - R_b^{\infty} \tag{44}$$

$$t_l \in [t_{b,0}, t_e],\ l \in \{n_{f,l}+1, \ldots, n_{b,l}\}. \tag{45}$$

$R_{f,l}(t_{n_{f,l}})$ is obtained from the solution of (P3).

The estimation of the parameters α and β is performed according to the algorithm proposed in the previous section (Figure 4). The problem formulation is analogous to (P3).

Optimal Control. The control problem, which employs the updated model, is

$$\min_{J_f, J_b, t_{\text{off}}, t_{f,e}, t_{b,e}} \phi \tag{P5}$$

$$\text{s.t. } \Delta p_j = J_j \cdot \eta \cdot R_j \tag{46}$$

$$R_f = R_f^0 + m \cdot J_f^{\alpha} \cdot u_c^{\beta} \cdot t \tag{47}$$

$$u_c = Q \cdot \frac{t_{\text{on}}}{t_{\text{on}} + t_{\text{off}}} \tag{48}$$

$$R_b = R_b^{\infty} + \Delta R \cdot n \cdot e^{-(t - t_{f,e})/(\tau_b)} \tag{49}$$

$$\Delta R = R_f(t_{f,e}) - R_b^{\infty} \tag{50}$$

$$J_{\text{net}} = \frac{J_f \cdot t_{f,e} - J_b \cdot (t_{b,e} - t_{f,e})}{t_e - t_0} \tag{51}$$

$$R_b(t_{b,e}) \le v \cdot R_b^{\infty}, v \ge 1 \tag{52}$$

$$J_f \le J_b \tag{53}$$

$$\Delta p_{\min} \le \Delta p \le \Delta p_{\max} \tag{54}$$

$$\mathbf{u}_{\min} \le \mathbf{u} \le \mathbf{u}_{\max} \tag{55}$$

$$t_0 = t_{f,0} \le t_{f,e} = t_{b,0} \le t_{b,e} = t_e \tag{56}$$

$$t \in [t_0, t_e],\ j = \begin{cases} f & \text{for } t \in [t_{f,0}, t_{f,e}] \\ b & \text{for } t \in [t_{b,0}, t_{b,e}]. \end{cases} \tag{57}$$

Equations 46–50 constitute the process model, where the differential equations for the filtration and backwashing resistance are replaced by their analytical solutions. The net flux J_{net} in Eq. 51 is considered a set-point specified by the operator or an upper level controller. Equation 52 forces the final resistance after the backwashing phase $R_b(t_{b,e})$ to be close to the irreversible resistance R_b^{∞}, introducing v as a tuning parameter. This way a sufficient cleaning of the membrane is realized in each cycle. The backwashing flux J_b is forced to be at least equal to the filtration flux J_f (Eq. 53), which is a common safety measure to limit pore blocking. Equations 54 and 55 give bounds on the TMP and on the manipulated variables J_f, J_b, $t_{f,e}$, $t_{b,e}$, and t_{off}. ϕ is defined according to Eq. 36.

Table 2. Tuning and Initial Model Parameters

Tuning Parameters			
ξ_1	2.5	ξ_2	200s
N	3	ε	5e−4
$q_{\max}^{\alpha}$	0.0625	$q_{\max}^{\beta}$	0.035
v	1.01		

Initial Model Parameters			
Filtration		Backwashing	
m	15e7	n	0.75
R_f^0	3e12	τ	1.25
α	1.5	R_b^{∞}	1.85e12
β	−1.5		

Simulation study

The performance of the controller is evaluated in a simulation study. The plant is replaced by a reference model,[4,8] which has been validated against plant measurements. The predictions obtained from the reference model are referred to as *simulated measurements*. The controller's tuning and initial model parameter values have been chosen according to Table 2. White noise with a standard deviation of 1% is added to the set-points of the manipulated variables. The model identification and set-point optimization are performed between two cycles, and the results are implemented in the next cycle without delay. Altogether, a sequence of 27 filtration cycles is considered. The simulated TMP measurements from the reference model and the TMP predictions from the controller are depicted in Figure 6, together with the relative error between the two. The respective values of the manipulated variables J_f, J_b, $\Delta t_f = t_{f,e}$, $\Delta t_b = t_{b,e} - t_{f,e}$, and t_{off}, as well as the net flux J_{net} are given in Figure 7. The interval length t_{on} with the aeration turned on is constant and set to $t_{\text{on}} = 12$s.

The simulation study is divided into two parts: during the first 12 cycles, the control loop is not closed, such that the controller has no influence on the process, which is operated with fixed values of the manipulated variables. In the open-loop part, the adaptation of the model in the presence of predefined changes in the operating conditions is evaluated (Figure 7). At cycle 4, the filtration flux J_f is increased, at cycle 7 the aeration pause t_{off} is changed from 12s to 48s, and at cycle 10 the backwashing flux J_b is increased. From cycle 13 on, the control loop is closed and the performance of the controller with respect to reliability and optimality is examined. The desired net flux J_{net} is specified and the

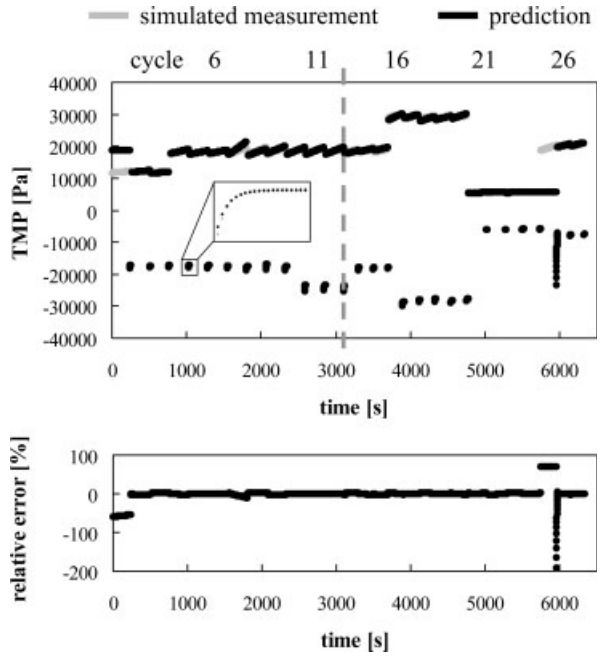

Figure 6. TMP measurements and prediction.

manipulated variables are computed by the controller (Figure 7). At cycle 16 the desired net flux J_{net} is increased, and at cycle 21 it is strongly decreased. At cycle 25, the membrane resistance in the reference model is strongly increased to simulate an unforeseen process disturbance. The according increase in TMP can be observed in Figure 6.

TMP Prediction and Model Adaptation. For most cycles, the controller's predictions are very close to the simulated measurements (Figure 6), even in the presence of large changes in the desired net flux J_{net}, e.g. at cycle 16 and cycle 21. The values of the updated parameters after each cycle are depicted in Figure 8. Only in three cycles the predictions deviate more than a few percent from the simulated measurements: the first cycle, cycle 7, and cycle 25. Each of these three instances is discussed in the following. The prediction for the first cycle is based on the model parameters that have been arbitrarily chosen according to Table 2. Accordingly, the prediction for the first cycle is arbitrarily bad. After the first cycle, the parameters are updated based on the obtained measurement data from cycle 1, and the prediction for cycle 2 is then very good.

At cycle 7, the aeration pause t_{off} is prolonged from 12s to 48s (Figure 7). In the model equations, the aeration intensity u_c has the exponent β (Eq. 27), which is not updated after each cycle due to the dual control problem. The initial value of β is -1.5 (Figure 8), which is too low. Hence, the TMP prediction after the set-point change of the aeration at cycle 7 deviates from the simulated measurement (Figure 6). However, the change of the aeration pause t_{off} (Figure 7) is exploited to update β to a value of about -0.7 (Figure 8), which in the following leads to good predictions even when the aeration intensity is changed (Figure 6). Likewise, α is adapted at a change of the filtration flux at cycle 4. It is observed that the filtration model parameter m is varying quite strongly during the first 9 cycles, but once α and β have been identified, m is relatively constant (Figure 8). This indicates that the filtration model structure is well chosen and that with properly identified parameters α and β, only small variations of the remaining model parameters can be expected.

The individual excitation of the inputs in the first 12 cycles facilitates the estimation of α and β. The tuning parameters related to the required confidence in the parameter estimates have been chosen tight, such that the subsequent excitation does not lead to a parameter update. Depending on the dynamics of the process, a less tight tuning and possibly deliberate excitation should allow for a more frequent update of these parameters.

At cycle 25, the simulated TMP measurement changes abruptly compared to the previous cycle (Figure 6) although the manipulated variables are almost the same (Figure 7). The reason is that the membrane resistance in the reference model has been strongly increased to simulate an unforeseen process disturbance. Naturally, the process disturbance is not predicted by the controller, which assumes the same process behavior as in the previous cycle. Hence, the TMP prediction differs strongly from the simulated measurements (Figure 6). After cycle 25, the model parameters are adapted (Figure 8), and from cycle 26 on the TMP prediction is very good again.

The analysis of the TMP prediction (Figure 6) shows that the proposed controller yields excellent results with respect to TMP prediction, even in the presence of large changes in the operating conditions and after a severe process disturbance. Based on this conclusion, the controller's performance with respect to process optimization is examined in the following.

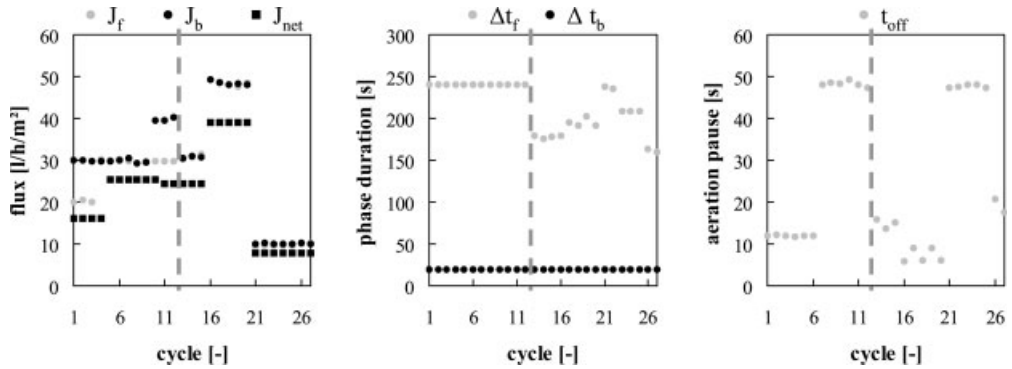

Figure 7. Manipulated variables and net flux.

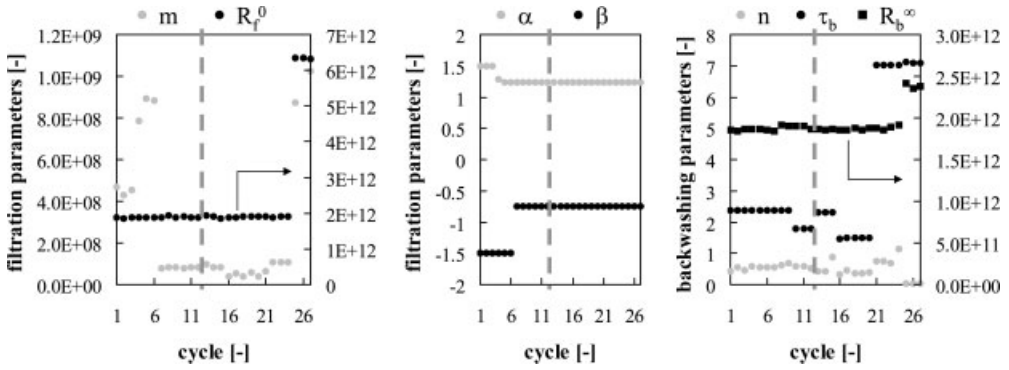

Figure 8. Model parameters as identified after each cycle.

Control Performance. From cycle 13 on, the control loop is closed and the optimal values of the manipulated variables as computed by the controller are implemented in the process (Figure 7). Although the desired net flux J_{net} does not change between the cycles 12 and 13, it is observed that the optimal values of the manipulated variables at cycle 13 are different from the fixed values in cycle 12. Most importantly, the aeration pause t_{off} is lowered from 48s to about 15s, which results in a smaller TMP increase during the cycles 13–15 (Figure 6). Also, the backwashing flux J_b is reduced.

At cycle 16, the net flux J_{net} is increased from about $25\frac{l}{h \cdot m^2}$ to $40\frac{l}{h \cdot m^2}$ (Figure 7). Accordingly, the filtration flux J_f and the backwashing flux J_b are increased by the controller, the filtration duration Δt_f is prolonged, and the aeration pause t_{off} is shortened. The latter is an obvious measure to decrease fouling, which is more severe at high fluxes. A longer duration of the filtration phase allows for a lower filtration flux, but on the other hand decreases the backwashing frequency.

When the desired net flux J_{net} is decreased to a low-value of about $8\frac{l}{h \cdot m^2}$ at cycle 21, the filtration and backwashing fluxes J_f and J_b are also decreased (Figure 7). The filtration phase duration Δt_f is first increased to about 240s, and then lowered back to 210s. The aeration pause is adjusted to its maximum value of 48s.

Finally, at cycle 25 the process is severely disturbed, which leads to a strong increase in measured TMP (Figure 6). The process model is adapted after cycle 25 (Figure 8), and the new values of the manipulated variables for cycle 26 already consider the new process behavior (Figure 7). The filtration phase duration Δt_f and the aeration pause t_{off} are strongly lowered to respond to the high TMP increase.

Qualitatively speaking, the values of the manipulated variables computed by the controller for a variety of operating conditions make perfect sense. In situations with high fluxes, fouling is a greater problem and needs to be counteracted by appropriately choosing the filtration duration length and by a higher aeration intensity. At very low fluxes, fouling is not a problem, which allows for long filtration phases and reduced aeration. In the given simulation study, the backwashing duration is always chosen to its minimum value of 20s, and the backwashing flux is always very close to the filtration flux, which is again a lower bound (Figure 7). This indicates, that the reversible fouling is completely removed under these conditions, which is confirmed by a close examination of the TMP evolution during backwashing (not shown). It is also observed in Figure 7 that the computed aeration pauses t_{off} vary for similar process conditions (cycles 16–20). The optimal aeration pause is quite sensitive to changes in the estimated model parameters. This can be circumvented by filtering the model parameters or the manipulated variables if the variation becomes too large.

In order to get an idea of the economical potential of the proposed run-to-run controller, it is compared against a typical choice of manipulated variables for the scenario considered above. For the cycles 13–27, a constant filtration duration $\Delta t_f = 240$s, backwashing duration $\Delta t_b = 20$s, and aeration pause $t_{off} = 12$s are assumed. The backwashing flux always equals the filtration flux, which is adapted to meet the desired net flux. The resulting TMP trajectories for the run-to-run control approach (Figure 6) and for the standard approach with fixed manipulated variables (not shown) are obtained from the reference model. The objective function is evaluated for both approaches based on the respective simulated measurements. The results are presented in Figure 9. For the cycles 1–12, the result is the same, as the control loop is not closed. For the cycles 13–20, the run-to-run controller yields up to 60% lower objective function values than the standard approach with fixed manipulated variables. This is especially true for the operation with high fluxes during the cycles 16–20. For the cycles 21–24, the standard approach and the run-to-run controller yield about the same objective function values. When the process disturbance occurs at cycle 25, the run-to-run controller performs slightly worse, but after model adaptation the controller again outperforms the standard approach.

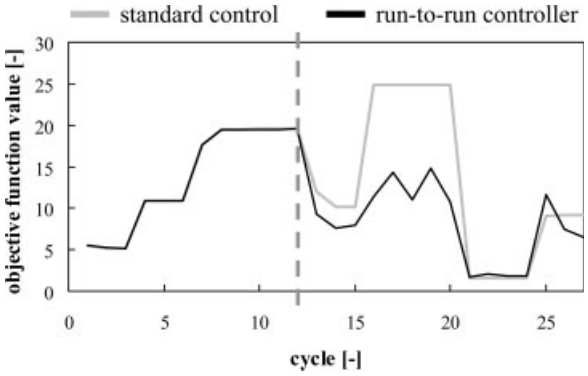

Figure 9. Objective function values for the standard approach and the run-to-run controller.

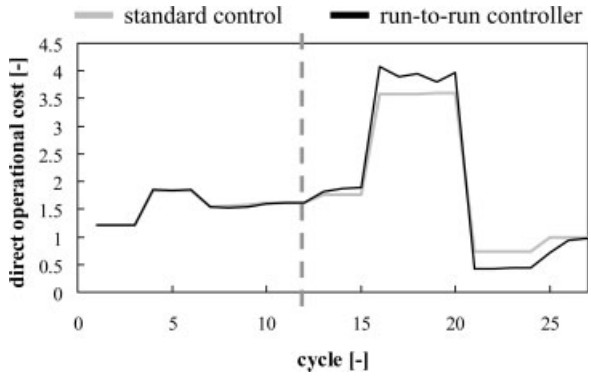

Figure 10. Operational cost without membrane replacement cost for the standard approach and the run-to-run controller.

The objective function (Eq. 36) considers the cost E_p to provide the TMP and the aeration cost E_c, which can both be predicted rigorously, and the membrane replacement cost E_r, which are predicted based on an empirical correlation. It is interesting to evaluate the rigorous part separately and observe how the controller affects the *direct operational cost* excluding membrane replacement cost. The result is depicted in Figure 10. During the cycles 13–15 and 26–27, the direct operational cost are about the same. During the cycles 16–20 with high fluxes, the direct operational cost are about 10% higher for the run-to-run controller. The high fouling caused by the high fluxes during these cycles is counteracted by the controller in order to lower the overall objective function by up to 60% (Figure 9). When fouling is very low during the cycles 21–24, the controller realizes the same overall cost (Figure 9), but the direct operational cost are reduced by about 40% (Figure 10).

To conclude, the run-to-run controller substantially lowers the overall cost of the process, reliably outperforming the standard approach with fixed set-points. When fouling is negligible, the direct operational cost are lowered by up to 40%, and when the fouling potential is high, the TMP increase is strongly lowered with an only slight increase in the direct operational cost. In addition, the run-to-run strategy updates the optimal set-points after each cycle and thereby reacts to process disturbances with only one cycle delay. Operational conditions, in which the membranes are strongly fouled and possibly damaged, are therefore avoided.

Conclusions

A generic methodology for the model-based control of membrane filtration processes is proposed, which is based on run-to-run control theory. It is exemplified for submerged membrane filtration in wastewater treatment applications, for which a suitable process model is developed. The controller is tested in a simulation scenario employing a rigorous and validated process model as plant substitution. It is shown to achieve excellent results concerning prediction quality, adaptation to process disturbances, and process optimization with respect to power consumption and irreversible membrane fouling.

The controller's performance is currently experimentally verified in an industrial pilot plant. One of the remaining challenging research topics is the rigorous modeling of the cost of membrane fouling in different applications, for which at the moment only empirical descriptions are available. Another research focus is the application of the proposed run-to-run controller to different industrial filtration applications.

Acknowledgments

The financial support by the DFG (German Research Foundation) in the project "Optimization-based process control of chemical processes" is gratefully acknowledged.

Notation

a = element of main axis of confidence ellipsoid
$\boldsymbol{a}$ = main axis of confidence ellipsoid
A = membrane area
$\mathbf{d}$ = vector of disturbances
E_p = power for permeate pumps, W
E_c = power for air compressor, W
E_r = membrane replacement cost
$\boldsymbol{H}$ = Hessian
J = flux, m s^{-1}
l = length of confidence ellipsoid axis
m = model parameter, Eq. 27
n = model parameter, Eq. 29
n = number of parameters/samples
N = number of cycles in estimation horizon
$\mathbf{p}$ = vector of parameters
$\hat{\mathbf{p}}$ = vector of estimated parameters
p_a = pressure difference across difference air compressor, bar
$\delta\boldsymbol{p}$ = parameter deviation
Δp = transmembrane pressure difference, Pa
$\Delta\tilde{p}$ = measured transmembrane pressure, Pa
q = uncertainty measure
Q = air flow rate, m^3 s^{-1}
$\mathbf{r}$ = vector of set-points from base control
R = resistance, m^{-1}
R_g = gas constant, J K^{-1} mol^{-1}
ΔR = reversible resistance m^{-1}
t = time, s
Δt = phase duration, s
T = set-point controlled variable
T = temperature, K
u = manipulated variable
$\mathbf{u}$ = vector of manipulated variables
u_c = cross-flow intensity
$\mathbf{v}$ = eigenvector
v_a = molar volume of air, m^3 mol^{-1}
$\mathbf{x}$ = vector of differential states
y = algebraic state
$\mathbf{y}$ = vector of algebraic states
$\tilde{\mathbf{y}}$ = vector of measured states

Greek letters

α = model parameter, Eqs. 2, 20, 27
β = model parameter, Eqs. 2, 20, 27
γ_a = polytropic coefficient
$\boldsymbol{\epsilon}$ = white noise
ε = indifference region parameter
η = viscosity, kg s^{-1} m^{-1}
η_A = efficiency factor, air compressor
η_P = efficiency factor, permeate pump
λ = eigenvalue
ν = parameter, Eq. 52
ξ_1 = parameter, Eq. 35
ξ_2 = parameter, Eq. 35
τ_b = model parameter, Eq. 29, s
ϕ = objective function

Subscripts

0 = beginning of time horizon
b = backwashing

e = end of time horizon
f = filtration
i = parameter index
j = phase index
l = sample index
max = maximum
min = minimum
net = net flow
off = aeration off
on = aeration on
p = all parameters
permeate = permeate side
r = parameters estimated on a longer horizon
s = parameters estimated on one cycle
slug = slug side

Superscripts

j = parameter index
k = cycle index
∞ = irreversible

Literature Cited

1. Choi H, Zhang K, Dionysiou DD, Oerther DB, Sorial GA. Influence of cross-flow velocity on membrane performance during filtration of biological suspension. *J Membrane Sci*. 2005;248:189–199.
2. Chen JP, Kim SL, Ting YP. Optimization of membrane physical and chemical cleaning by a statistically designed approach. *J Membrane Sci*. 2003;219:27–45.
3. Jiang T, Kennedy MD, Guinzbourg BF, Vanrolleghem PA, Schippers JC. Optimising the operation of a MBR pilot plant by quantitative analysis of the membrane fouling mechanism. *Water Sci Technol*. 2005;51:19–25.
4. Busch J, Cruse A, Marquardt W. Modeling submerged hollow-fiber membrane filtration for wastewater treatment. *J Membrane Sci*. 2006; 288:94–111.
5. Hwang K-J, Yu Y-H, Lu W-M. Cross-flow microfiltration of submicron microbial suspension. *J Membrane Sci*. 2001;194:229–243.
6. Smith PJ, Vigneswaran S, Ngo HN, Ben-Anim R, Nguyen H. A new approach to backwash initiation in membrane systems. *J Membrane Sci*. 2006;278:381–389.
7. Blankert B, Betlem BHL, Roffel B. Dynamic optimization of a dead-end filtration trajectory: Blocking filtration laws. *J Membrane Sci*. 2006;285:90–95.
8. Broeckmann A, Busch J, Wintgens T, Marquardt W. Modeling of pore blocking and cake layer formation in membrane filtration for wastewater treatment. *Desalination*. 2006;189:97–109.
9. Polyakov YS. Deadend outside-in hollow-fiber membrane filter: Mathematical model. *J Membrane Sci*. 2006;279:615–624.
10. Gehlert G, Abdulkadir M, Fuhrmann J, Hapke J. Dynamic modeling of an ultrafiltration module for use in a membrane bioreactor. *J Membrane Sci*. 2005;248:63–71.
11. Marriott J, Sørensen E. A general approach to modelling membrane modules. *Chem Eng Sci*. 2003;58:4975–4990.
12. Marriott J, Sørensen E. The optimal design of membrane systems. *Chem Eng Sci*. 2003;58:4991–5004.
13. Mangold M, Ginkel M, Gilles ED. A model library for membrane reactors implemented in the process modelling tool PROMOT. *Comput Chem Eng*. 2004;28:319–332.
14. Hermia J. Constant pressure blocking filtration laws - Application to power- law non-newtonian fluids. *T I Chem Eng-Lon*. 1982;60:183–187.
15. Chellam S. Artificial neural network for transient crossflow microfiltration of polydispersed suspensions. *J Membrane Sci*. 2005;258:35–42.
16. Katsikaris K, Boukouvalas C, Magoulas K. Simulation of ultrafiltration process and application to pilot tests. *Desalination*. 2005;171:1–11.
17. Geissler S, Wintgens T, Melin T, Vossenkaul K, Kullmann C. Modelling approaches for filtration processes with novel submerged capillary modules in membrane bioreactors for wastewater treatment. *Desalination*. 2005;178:125–134.
18. Castillo E, Hurwitz AM. Run-to-run process control: Literature review and extensions. *J Qual. Technol*. 1997;29:184–196.
19. Castillo E, Yeh J-Y. An adaptive run-to-run optimizing controller for linear and nonlinear semiconductor processes. *IEEE T Semiconduct, M*. 1998;11:285–295.
20. Patel NS, Jenkins ST. Adaptive optimization of run-to-run controllers: The EWMA example. *IEEE T Semiconduct, M*. 2000;13:97–107.
21. Srinivasan B, Bonvin D. Interplay between identification and optimization in run-to-run optimization schemes. In: Proceedings of the American Control Conference (Anchorage); 2002:2174–2179.
22. Zhang C, Deng H, Baras JS. Run-to-run control methods based on the DHOBE alogrithm. *Automatica*. 2003;39:35–45.
23. Gao W, Engell S. Iterative set-point optimization of batch chromatography. *In: ESCAPE*. 2004;14:661–667.
24. Bonné D, Jørgensen SB. Batch to batch improving control of yeast fermentation. In: *ESCAPE*. 2001;11:621–626.
25. Xiong Z, Zhang J. A batch-to-batch iterative optimal control strategy based on recurrent neural network models. *J Process Contr*. 2005;15:11–21.
26. Srinivasan B, Primus CJ, Bonvin D, Ricker NL. Run-to-run optimization via control of generalized constraints. *Control Eng Pract*. 2001;9:911–919.
27. François G, Srinivasan B, Bonvin D, Barajas JH, Hunkeler D. Run-to-run adaptation of a semiadiabatic policy for the optimization of an industrial batch polymerization process. *Ind Eng Chem Res*. 2004;43:7238–7242.
28. Vassiliadis VS, Sargent RWH, Pantelides CC. Solution of a class of multistage dynamic optimization problems. 2. Problems with path constraints. *Ind Eng Chem Res*. 1994;33:2123–2133.
29. Oldenburg J, Marquardt W, Heinz D, Leineweber DB. Mixed-logic dynamic optimization applied to batch distillation process design. *AIChE J*. 2003;49:2900–2917.
30. Bard Y. Nonlinear Parameter Estimation. New York and London: Academic Press; 1974.
31. Rao CV, Rawlings JB, Mayne DQ. Constrained state estimation for nonlinear discrete-time systems: stability and moving horizon approximations. *IEEE T Automat. Contr*. 2003;48:246–258.
32. Ljung L. System Identification. Englewood Cliffs: Prentice Hall; 1987.
33. Wittenmark B. Adaptive dual control methods: An overview. In: *5th IFAC Symposium on Adaptive Systems in Control and Signal Processing*; 1995:67–73.
34. Roberts PD. An algorithm for steady-state system optimization and parameter estimation. *Int J Systems Sci*. 1979;10:719–734.
35. Roberts PD. Coping with model-reality differences in industrial process optimisation – A review of integrated system optimisation and parameter estimation. *Comput Ind*. 1995;26:281–290.
36. Findeisen R, Allgöwer F. Computational delay in nonlinear model predictive control. In: *Proc Int Symp Adv Control of Chemical Processes*; 2003.
37. Gray NF. *Biology of Wastewater Treatment; No 4 of Series on Environmental Science and Management*. Imperial College Press; 2004.
38. Wintgens T, Melin T, Schäfer A, Khan S, Muston M, Bixio D, Thoeye C. The role of membrane processes in municipal wastewater treatment reclamation and reuse. *Desalination*. 2005;178:1–11.
39. Husain H, Côté P. Membrane bioreactors for municipal wastewater treatment. *Wat Qual Int*. 1999;March/April:19–22.
40. Engelhardt N, Firk W, Warnken W. Integration of membrane filtration into the activated sludge process in municipal wastewater treatment. *Wat Sc Tech*. 1998;38:429–436.
41. Stephenson T, Brindle K, Judd S, Jefferson B. *Membrane Bioreactors for Wastewater Treatment*. IWA Publishing; 2000.
42. Yang W, Cicek N, Ilg J. State-of-the-art of membrane bioreactors: Worldwide research and commercial applications in North America. *J Membrane Sci*. 2006;270:201–211.
43. Lübbecke S, Vogelpohl A. Wastewater treatment in a biological high-performance system with high biomass concentration. *Water Res*. 1995;29:793–802.

Manuscript received Aug. 14, 2006, and revision received Apr. 16, 2007.